Modulation transfer function of hexagonal staring focal plane arrays

Kenneth J. Barnard, MEMBER SPIE
Glenn D. Boreman, MEMBER SPIE
University of Central Florida
Electrical Engineering Department
Center for Research in Electro-Optics and Lasers
Orlando, Florida 32816

Abstract. The modulation transfer functions (MTFs) of hexagonally sampled arrays with both rectangular and hexagonal pixel shapes are derived from spatial averaging considerations. In one direction, the hexagonal pixel shape is shown to provide a 13.6% improvement in MTF at the Nyquist bandlimit over an equivalent rectangular shape. For the orthogonal direction, the hexagonal shape has a slightly worse MTF, which is 4.8% less than the MTF of the rectangular shape at the Nyquist bandlimit.

Subject terms: modulation transfer function; hexagonal sampling; hexagonal detector arrays; infrared focal plane arrays.

Optical Engineering 30(12), 1915-1919 (December 1991).

CONTENTS

1. INTRODUCTION

Hexagonal sampling for detector arrays can provide an improvement over rectangular sampling. For circularly bandlimited two-dimensional signals with circular support, the hexagonal sampling lattice is optimal in the sense that a lower sampling density is required for exact reconstruction of the signal.[1–3] Hexagonal sampling requires approximately 13.4% fewer samples than rectangular sampling. In point-source tracking applications, hexagonal sampling with a hexagonal pixel shape also has advantages over rectangular sampling.[4–6] For point-source location, the hexagonal detector array gives a lower error for the centroid calculation and the algorithm is also less sensitive to detector noise.

This paper considers hexagonally sampled detector arrays in terms of their modulation transfer function (MTF). An expression for the MTF is derived by treating the array as an integral sampler. An integral sampler produces a sampled version of the input irradiance by first performing spatial averaging of the input irradiance over the individual pixels, followed by a point-sampling process. For bandlimited input irradiance functions, the MTF can be derived from the geometrical shape of individual pixels. The MTFs for both hexagonal pixels and equivalent-area rectangular pixels are calculated. A hexagonal pixel shape is shown to have an additional advantage over a rectangular pixel shape in terms of the MTF.

Paper 13011 received Jan. 17, 1991; revised manuscript received June 18, 1991; accepted for publication June 18, 1991.

2. MTF DEPENDENCE ON PIXEL SHAPE

Figure 1 shows the hexagonal and equivalent rectangular pixel shapes for a small portion of a hexagonally sampled detector array. Two assumptions were made regarding the detector array geometry. First, a 100% fill factor was used to simplify the analysis. Second, a regular hexagonal shape with a side length of L was used to produce the detector array; the sampling lattice coordinates were determined from this construction. The rectangular pixel shape and the hexagonal pixel shape shown in Fig. 1 have equal areas and have the same sampling lattice points.

The hexagonal sampling lattice can be expressed as the two-dimensional comb function[7]:

$$\operatorname{samp}(x,y)=\operatorname{comb}\left(\frac{x}{3L}+\frac{y}{\sqrt{3}L}\,,\ \frac{x}{3L}-\frac{y}{\sqrt{3}L}\right) \tag{1}$$

$$=\frac{3\sqrt{3}L^2}{2}\sum_{n=-\infty}^{\infty}\sum_{m=-\infty}^{\infty}\delta\left[x-\left(\frac{3L}{2}n+\frac{3L}{2}m\right)\right]\times\delta\left[y-\left(\frac{\sqrt{3}L}{2}n-\frac{\sqrt{3}L}{2}m\right)\right], \tag{2}$$

which is shown in Fig. 1 over a small portion of the x-y plane. An input irradiance function, $i(x,y)$, can be exactly reconstructed from its hexagonally sampled version if it is bandlimited within a hexagonal region in the spatial frequency domain.[1] To simplify the analysis, we assume that the input irradiance function is bandlimited in a circular region inscribed within the hexagonal bandlimited region required by the sampling function. The bandlimit placed on the input irradiance function can be expressed as

$$I(\xi,\eta)=0 \quad \text{if } \xi^2+\eta^2>\left(\frac{1}{3L}\right)^2 . \tag{3}$$

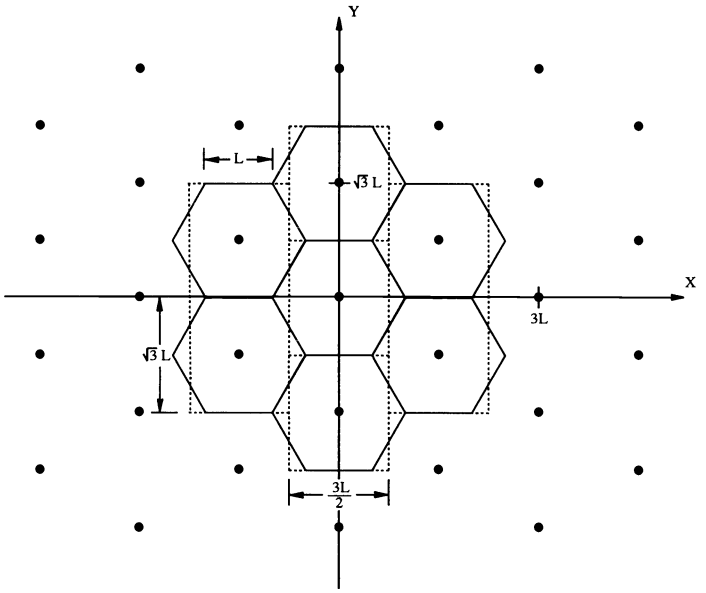

Fig. 1. Hexagonal and equivalent-area rectangular pixels in a hexagonal array.

The sampled version, $r(x,y)$, of the input irradiance function for a hexagonally sampled array with rectangular pixels is obtained by averaging the input irradiance function over the pixel areas and then performing delta-function sampling at the center of each pixel. This is called an *integral sampling process*[8] and can be written as

$$r(x,y)=k\left[i(x,y)**\text{rect}\left(\frac{x}{3L/2},\frac{y}{\sqrt{3}L}\right)\right]\times\left[\text{comb}\left(\frac{x}{3L}+\frac{y}{\sqrt{3}L},\frac{x}{3L}-\frac{y}{\sqrt{3}L}\right)\right]\times\text{rect}\left(\frac{x}{W},\frac{y}{W}\right), \tag{4}$$

where k is a constant, $i(x,y)$ is the input irradiance function, and $W\times W$ is the dimension of the array. The spectrum of $r(x,y)$ is obtained by Fourier transformation:

$$R(\xi,\eta)=k\left[I(\xi,\eta)\text{sinc}\left(\frac{3L}{2}\xi,\sqrt{3}L\eta\right)\right]**\text{comb}\left(\frac{3L}{2}\xi+\frac{\sqrt{3}L}{2}\eta,\frac{3L}{2}\xi-\frac{\sqrt{3}L}{2}\eta\right)**\text{sinc}(W\xi,W\eta), \tag{5}$$

where $I(\xi,\eta)$ is the spectrum of the input irradiance. Because the input irradiance function is bandlimited, that is, no aliasing occurs, we can disregard all of the delta functions comprising the comb except the one at the origin. Also, in the approximation $W>>L$, $\text{sinc}(W\xi,W\eta)$ can be approximated by $\delta(\xi,\eta)$. With these assumptions, $R(\xi,\eta)$ can be written as

$$R(\xi,\eta)\approx kI(\xi,\eta)\text{sinc}\left(\frac{3L}{2}\xi,\sqrt{3}L\eta\right). \tag{6}$$

The MTF is defined as the ratio of the spectrum of the output to the spectrum of the input, normalized to unity at zero spatial frequency:

$$\text{MTF}(\xi,\eta)=\frac{R(\xi,\eta)/I(\xi,\eta)}{R(0,0)/I(0,0)}. \tag{7}$$

Thus, for a hexagonal array of rectangular pixels, the MTF is given by

$$\text{MTF}(\xi,\eta)\approx\text{sinc}\left(\frac{3L}{2}\xi,\sqrt{3}L\eta\right). \tag{8}$$

Taking the slices $\eta=0$ and $\xi=0$ through the MTF gives the MTF in the x and y directions, respectively. These can be written as

$$\text{MTF}(\xi)\approx\text{sinc}\left(\frac{3L}{2}\xi\right), \tag{9}$$

$$\text{MTF}(\eta)\approx\text{sinc}(\sqrt{3}L\eta). \tag{10}$$

Following a similar analysis, we can derive the MTF for a hexagonally sampled array with hexagonal pixels. The sampled input irradiance function for this case can be written as

$$r(x,y)=k[i(x,y)**d(x,y)]\left[\text{comb}\left(\frac{x}{3L}+\frac{y}{\sqrt{3}L},\frac{x}{3L}-\frac{y}{\sqrt{3}L}\right)\right]\times\text{rect}\left(\frac{x}{W},\frac{y}{W}\right), \tag{11}$$

where the rectangular detector shape in Eq. (4) has been replaced with a hexagonal detector shape $d(x,y)$. Taking the Fourier transform of Eq. (11) gives the spectrum of the response:

$$R(\xi,\eta)=k[I(\xi,\eta)D(\xi,\eta)]**\text{comb}\left(\frac{3L}{2}\xi+\frac{\sqrt{3}L}{2}\eta,\frac{3L}{2}\xi-\frac{\sqrt{3}L}{2}\eta\right)**\text{sinc}(W\xi,W\eta). \tag{12}$$

Using the same approximations that led to Eq. (6), we can write the response spectrum as

$$R(\xi,\eta)\approx kI(\xi,\eta)D(\xi,\eta). \tag{13}$$

By the definition of MTF given in Eq. (7), the two-dimensional MTF of the hexagonal detector array is

$$\text{MTF}(\xi,\eta)\approx\frac{D(\xi,\eta)}{D(0,0)}, \tag{14}$$

The MTF along $\eta=0$ and $\xi=0$ requires knowledge of $D(\xi,0)$ and $D(0,\eta)$. The hexagonal detector shape, $d(x,y)$, is a nonseparable one-zero function, which implies

$$D(\xi,0)\neq\mathcal{F}[\text{d}(x,0)], \tag{15a}$$

$$D(0,\eta)\neq\mathcal{F}[d(0,y)]. \tag{15b}$$

Because the detector shape is symmetric about x and y, the

necessary Fourier transforms can be obtained from the x and y profiles of $d(x,y)$.[9] The profiles $d_y(x)$ and $d_x(y)$, of the hexagon shape are shown in Figs. 2 and 3, respectively. Using the formulation in Ref. 9, the MTF along $\eta=0$ and $\xi=0$ can be written as

$$\mathrm{MTF}(\xi)\approx\frac{D(\xi,0)}{D(0,0)}=\frac{D_y(\xi)}{D_y(0)}\ , \tag{16}$$

$$\mathrm{MTF}(\eta)\approx\frac{D(0,\eta)}{D(0,0)}=\frac{D_x(\eta)}{D_x(0)}\ . \tag{17}$$

To compute $D_y(\xi)$, we note that the x profile shown in Fig. 2 can be written as

$$d_y(x)=k\left[\mathrm{rect}\left(\frac{x}{L/2}\right)*\mathrm{rect}\left(\frac{x}{3L/2}\right)\right]\ , \tag{18}$$

and the corresponding Fourier transform for $d_y(x)$ is

$$D_y(\xi)=k\ \mathrm{sinc}\left(\frac{L}{2}\xi\right)\ \mathrm{sinc}\left(\frac{3L}{2}\xi\right)\ . \tag{19}$$

The MTF along the x direction is then given by Eq. 16 as

$$\mathrm{MTF}(\xi)\approx\mathrm{sinc}\left(\frac{L}{2}\xi\right)\ \mathrm{sinc}\left(\frac{3L}{2}\xi\right)\ . \tag{20}$$

The MTF along the y direction can be computed similarly. The y profile of the detector shape shown in Fig. 3 can be written as

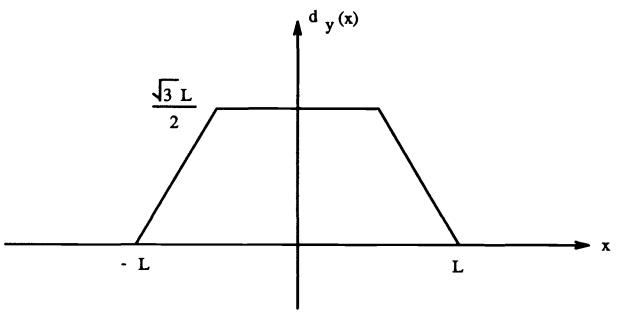

Fig. 2. Hexagonal pixel shape in the *x* direction.

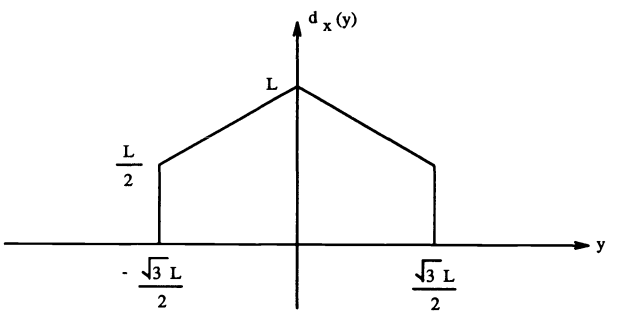

Fig. 3. Hexagonal pixel shape in the *y* direction.

$$d_x(y)=k\left[\mathrm{tri}\left(\frac{y}{\sqrt{3}L/2}\right)+\mathrm{rect}\left(\frac{y}{\sqrt{3}L}\right)\right]\ , \tag{21}$$

which has the Fourier transform

$$D_x(\eta)=k\left[\mathrm{sinc}(\sqrt{3}L\eta)+\frac{1}{2}\ \mathrm{sinc}^2\left(\frac{\sqrt{3}L}{2}\eta\right)\right]\ . \tag{22}$$

The resulting MTF along the y direction is, by Eq. (17),

$$\mathrm{MTF}(\eta)\approx\frac{2}{3}\left[\mathrm{sinc}(\sqrt{3}L\eta)+\frac{1}{2}\ \mathrm{sinc}^2\left(\frac{\sqrt{3}L}{2}\eta\right)\right]\ . \tag{23}$$

These MTF results for the hexagonal pixel shape are consistent with the more general analysis performed in Refs. 10 and 11.

The MTF along the x direction of the hexagonally sampled array is shown in Fig. 4 for both rectangular and hexagonal pixel shapes. The Nyquist bandlimit represents the upper frequency limit of the input irradiance function to avoid aliasing. Figure 4 shows that in the x direction the MTF for the hexagonal-pixel-shape array is approximately 4.8% worse than for the rectangular-pixel-shape array at the Nyquist bandlimit. However, the y direction MTF shown in Fig. 5 shows an improvement of approximately 13.6% in MTF for the hexagonal-pixel-shape array at the Nyquist bandlimit. Inspection of Figs. 4 and 5 indicates that the MTF resulting from a hexagonal pixel shape is almost identical in the x and y directions out to the Nyquist bandlimit.

To further quantify the comparison of the MTF of hexagonal and rectangular pixel shapes, two-dimensional MTFs of these structures were calculated. These are shown in Figs. 6 and 7 for the rectangular and hexagonal pixel shapes, respectively. The MTFs shown in these figures extend beyond the Nyquist bandlimit to illustrate the differences between the two functions. Over the bandlimited spatial frequency region of interest, an MTF difference function (Hex. MTF − Rect. MTF) was formed to show the difference between the two MTFs. The contour plot of this difference function is given in Fig. 8. The hexagonal pixel shape MTF exceeds the MTF of the rectangular pixel shape over most of the bandlimited region.

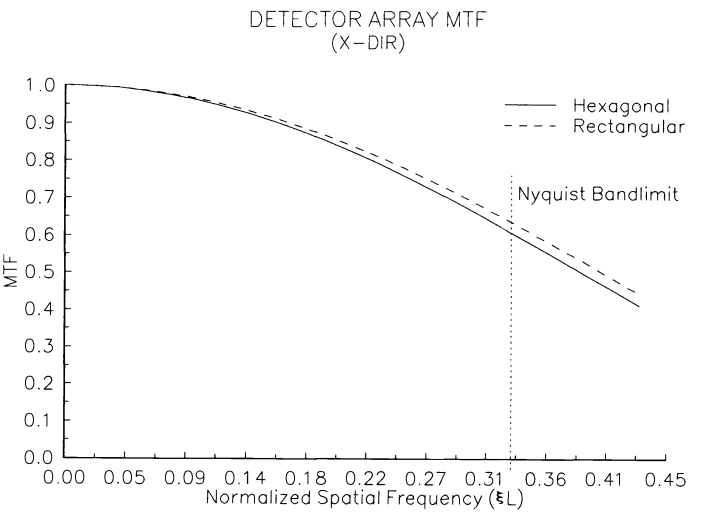

Fig. 4. MTF in the *x* direction for hexagonally sampled detector array.

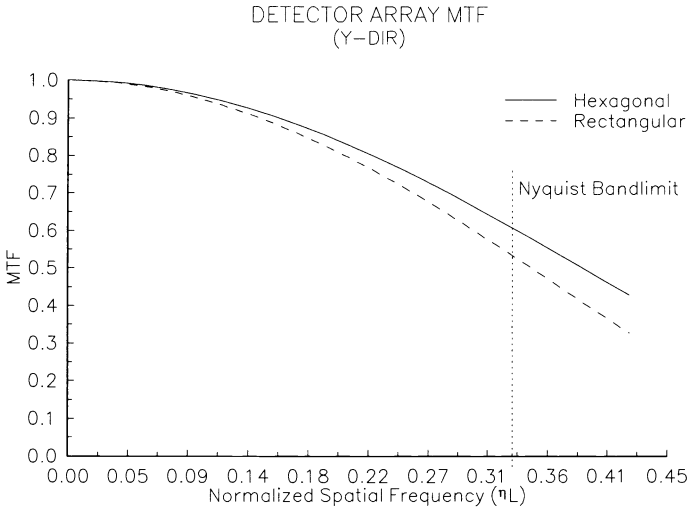

Fig. 5. MTF in the *y* direction for hexagonally sampled detector array.

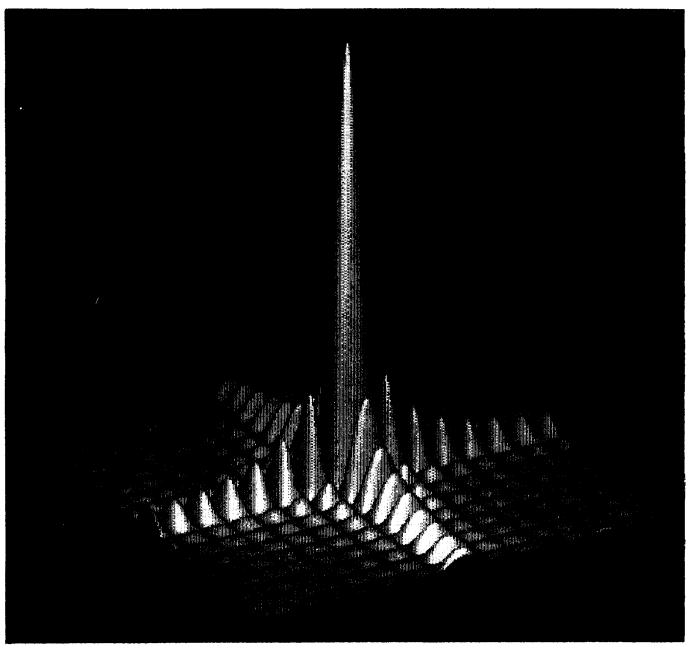

Fig. 6. Two-dimensional MTF of rectangular pixel shape.

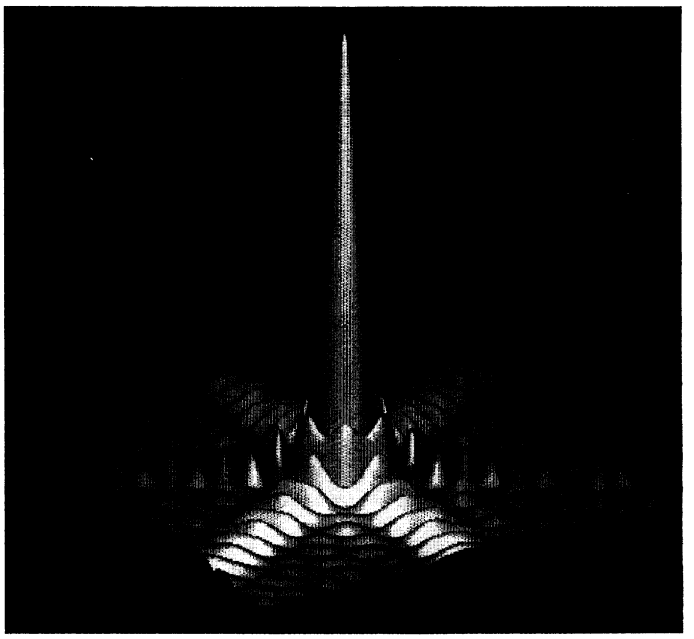

Fig. 7. Two-dimensional MTF of hexagonal pixel shape.

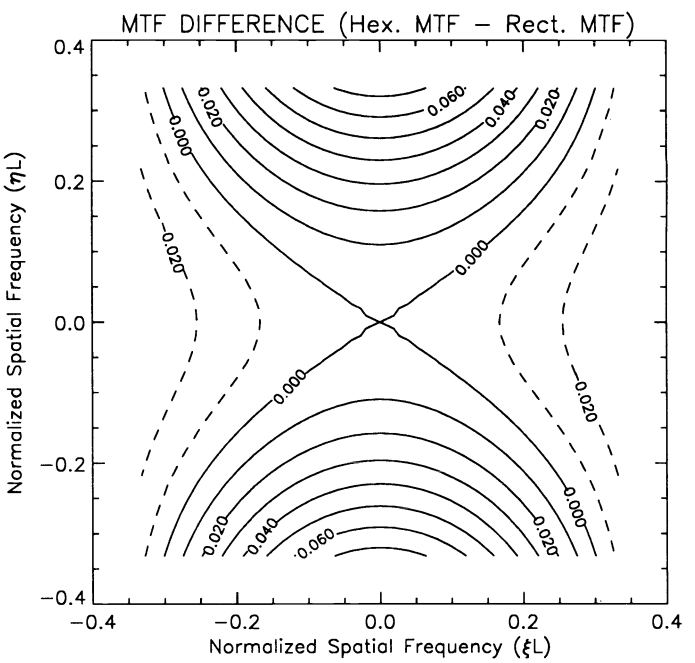

Fig. 8. Contour plot of the MTF difference of the hexagonal pixel shape and the rectangular pixel shape (solid lines are positive, dotted are negative).

3. CONCLUSIONS

The hexagonally sampled focal plane array was found to have an MTF that is strictly dependent on pixel geometry. For hexagonal and equivalent-area rectangular pixel shapes, the MTF was found in closed form, and it was shown that x and y cross sections of the MTF are not equivalent for the two pixel shapes. In the x direction, the MTF resulting from a hexagonal pixel shape is approximately 4.8% worse than for a rectangular pixel shape at the Nyquist bandlimit. The y direction MTF for the hexagonal pixel shape is approximately 13.6% better than the rectangular pixel shape at the Nyquist bandlimit. The MTF of the hexagonal pixel shape is approximately equivalent in both x and y directions up to the Nyquist bandlimit, and a two-dimensional analysis indicates that the hexagonal-pixel-shape MTF exceeds that of the rectangular-pixel-shape MTF over most of the bandlimited region.

4. ACKNOWLEDGMENT

This work was supported by the Office of Naval Research/SDIO-IST under Contract N0014-89-K-0125.

5. REFERENCES

1. R. Mersereau, "The processing of hexagonally sampled two-dimensional signals," *Proc. IEEE* **67**, 930–949 (1979).
2. R. Mersereau, "Hexagonal pixels, arrays, and sampling," in *Infrared Systems and Components*, R. L. Caswell, ed., *Proc. SPIE* **750**, 57–61 (1987).
3. J. Hynecek, "A new device architecture suitable for high-resolution and high-performance image sensors," *IEEE Trans. Electron Devices* **35**, 646–652 (1988).

4. J. Cox, "Advantages of hexagonal detectors and variable focus for point-source sensors," *Opt. Eng.* **28**(11), 1145–1150 (1989).
5. J. Cox, "Point-source location using hexagonal detector arrays," *Opt. Eng.* **26**(1), 69–74 (1987).
6. J. Cox, "Point source location sensitivity analysis," in *Infrared Detectors, Sensors, and Focal Plane Arrays,* H. Nakamura, ed., *Proc. SPIE* **686**, 130–137 (1986).
7. J. Gaskill, *Linear Systems, Fourier Transforms, and Optics,* pp. 91–94, 279–285, Wiley, New York (1978).
8. F. Chazallet, J. Glasser, J. Vaillant, "Theoretical bases and measurement of the MTF for integrated image sensors," *Proc. SPIE* **702**, 175–178 (1986).
9. G. Boreman and A. Plogstedt, "Spatial filtering by a line-scanned nonrectangular detector: application to SPRITE readout MTF," *Appl. Opt.* **28**(6), 1165–1168 (1989).
10. D. P. Petersen and D. Middleton, "Sampling and reconstruction of wave-number-limited functions in N-dimensional euclidean spaces," *Inform. Contr.* **5**, 279–323 (1962).
11. R. C. Smith and J. S. Marsh, "Diffraction patterns of simple apertures," *J. Opt. Soc. Am.* **64,** 798–803 (1974).

Kenneth J. Barnard received the BS degree in electrical engineering from the University of Michigan in 1986 and is currently pursuing a Ph.D. degree in electrical engineering at the University of Central Florida (UCF). He previously held a technical staff position at General Dynamics Land Systems. Mr. Barnard is a graduate research assistant at the Center for Research in Electro-Optics and Lasers (CREOL) at UCF. He is a member of SPIE, IEEE, and OSA.

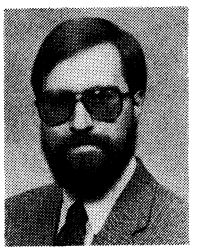

Glenn D. Boreman received the BS degree in optics from the University of Rochester in 1978 and the Ph.D. degree in optical sciences from the University of Arizona in 1984. He has held visiting technical staff positions at ITT, Texas Instruments, U.S. Army Night Vision Laboratory, and McDonnell Douglas. Dr. Boreman has been at the University of Central Florida since 1984 and is currently an associate professor of electrical engineering. He is a member of OSA, IEEE, SPIE, and SPSE and is a past president of the Florida section of OSA.